Int. J. Heat Mass Transfer. Vol. 2, pp. 106–120. Pergamon Press 1961. Printed in Great Britain.

NATURAL CONVECTION IN AN AIR LAYER ENCLOSED BETWEEN TWO VERTICAL PLATES WITH DIFFERENT TEMPERATURES*

E. R. G. ECKERT† and WALTER O. CARLSON‡

Heat Transfer Laboratory, University of Minnesota, Minneapolis, Minn., U.S.A.

(*Received* 22 *January* 1960)

Abstract—The temperature field in an air layer enclosed between two isothermal vertical plates with different temperatures has been investigated with the help of a Zehnder–Mach interferometer. Local heat transfer coefficients were derived from the temperature gradients in the air normal to the plate surfaces. Below a certain Grashof number and above a certain value of the height to thickness ratio, heat is transferred from the hot to the cold boundary by conduction in the central part of the layer. Convection contributes only in the corner regions. For large Grashof numbers and below a certain limit of the height to thickness ratio, boundary layers exist along the surfaces of the enclosure, whereas in the central core the temperature is uniform in horizontal planes. The temperature increases, however, in vertical direction. Fluctuations in the flow and wave motions were observed in some of the experiments. Relations for local and average heat transfer are presented.

Résumé—Le champ termique d'une couche d'air comprise entre deux plaques verticales isothermes ayant des températures différentes a été étudié au moyen d'un interféromètre de Mach–Zehnder. Les coefficients locaux de transmission de chaleur ont été déterminés à partir des gradients de température de l'air, perpendiculaires aux plaques. Au-dessous d'un certain nombre de Grashof et au-dessus d'une certaine valeur du rapport hauteur/épaisseur, la chaleur se transmet par conduction dans la partie centrale de la couche, de la frontière chaude à la frontière froide. La convection n'intervient que près des angles. Pour de grands nombres de Grashof et au-dessous d'une certaine limite du rapport hauteur/épaisseur, des couches limites existent le long des surfaces de l'enceinte, alors que dans la partie centrale la température est uniforme dans des plans horizontaux. Cependant, la température croît suivant la verticale. Des fluctuations dans l'écoulement et des mouvements d'ondes ont été observés dans quelques unes des expériences. Des relations pour la transmission de chaleur moyenne et locale sont présentées.

Zusammenfassung—Das Temperaturfeld einer Luftschicht zwischen zwei senkrechten, verschieden temperierten Platten wurde mit Hilfe des Zehnder–Mach-Interferometers untersucht. Aus den Temperaturgradienten der Luft normal zur Plattenoberfläche wurden örtliche Wärmeübergangskoeffizienten abgeleitet. Unterhalb einer gewissen Grashofzahl und oberhalb eines gewissen Verhältnisses Höhe zu Breite wird Wärme im Mittelteil nur durch Leitung übertragen und nur in den Ecken auch durch Konvektion. Für grosse Grashofzahlen und oberhalb einer gewissen Grenze des Höhe-Breite-Verhältnisses existiert eine Grenzschicht längs der Schichtoberflächen, während im Mittelteil die Temperatur in horizontalen Ebenen gleichförmig ist, in senkrechter Richtung aber ansteigt. Bei einigen Versuchen wurden fluktuierende Strömung und Wellenbewegungen beobachtet. Beziehungen für den örtlichen und mittleren Wärmeübergang werden angegeben.

Аннотация—Исследовалось температурное поле в слое воздуха между двумя изотермическими вертикальными пластинами при разных температурах посредством интерферометра Цендера-Маха. Локальные коэффициенты теплообмена получены путем вычисления температурных градиентов в слое воздуха в направлении, перпендикулярном к поверхности пластины. Показано, что ниже определенного значения критерия Грасгофа и больше данного предела параметрического критерия отношения высоты к толщине слоя, перенос тепла от горячей к холодной границе происходит путем теплопроводности в центральной части слоя. Конвекция имеет место только в

* The paper is an extension of a Ph.D. thesis by Walter O. Carlson [1].

† Professor of Mechanical Engineering, University of Minnesota.

‡ Leader, Physics Group, Radio Corporation of America, Moorestown, New Jersey.

угловых областях. Для больших чисел Грасгофа и ниже данного предела отношения высота к толщине слоя пограничные слом существуют только вдоль поверхностей, тогда как в центральном сечении температура равномерна в горизонтальных плоскостях. Однако, температура увеличивается в вертикальном направлении. В некоторых опытах наблюдались волны флюктуации в движениях потока. Приводятся данные по локальным и осредненным значениям коэффициентов теплообмена.

NOMENCLATURE

C, constant;
g, gravitational acceleration;
H, height of air layer;
$h = \frac{q}{T_H - T_C}$ heat transfer coefficient;
$h' = \frac{q}{T_w - T_m}$ heat transfer coefficient;
k, thermal conductivity;
L, thickness of air layer;
m, exponent;
n, exponent;
q, heat flow per unit area and time;
T, temperature;
W, width of air layer;
x, distance from corner;
x_p depth of penetration;
y, distance from wall
α, thermal diffusivity;
β, thermal expansion coefficient;
ν, kinematic viscosity;
δ, boundary layer thickness.

Indices

c, center region;
C, cold;
d, departure corner;
H, hot or based on height;
L, based on L;
m, centerline;
s, starting corner;
w, wall (either hot or cold);
x, based on x;
—, indicates average value.

Dimensionless parameters:

$Gr_L = \frac{g\beta(T_H - T_C)L^3}{\nu^2}$ Grashof number based on L;
$Gr_x = \frac{g\beta(T_H - T_C)x^3}{\nu^2}$ Grashof number based on x;
$Gr_H = \frac{g\beta(T_H - T_C)H^3}{\nu^2}$ Grashof number based on H;
$Gr'_x = \frac{g\beta(T_w - T_m)x^3}{\nu^2}$ Grashof number based on $T_w - T_m$ and x;
$Nu_L = \frac{hL}{k}$ Nusselt number based on L;
$Nu_x = \frac{hx}{k}$ Nusselt number based on x;
$\overline{Nu}_H = \frac{\bar{h}H}{k}$ average Nusselt number based on H;
$Nu'_x = \frac{h'x}{k}$ Nusselt number based on h' and x;
$Pr = \frac{\nu}{\alpha}$ Prandtl number;
$Ra = (Gr)(Pr)$ Rayleigh number.

INTRODUCTION

AIR layers enclosed between two vertical plates with different temperatures are used in many engineering applications as a means to decrease a heat flux and the corresponding heat losses. Natural convection arising in such layers limits the insulating effect. In other applications, the convection in the enclosed fluid is utilized to transport heat. Accordingly, the problem of predicting the amount of heat transported through such a layer has found considerable attention in the past. A first publication [2] on this subject by W. Nusselt in 1909 was followed by a series of other papers [3–11] reporting on experimental studies. The most extensive ones are the papers by Mull and Reiher [4] and by De Graaf and van der Held [10]. The aim of these studies was primarily to measure the amount of heat which is transported from the hot to the cold plate in such a geometry. The results, as far as they were presented by dimensionless relations, were put into the form

$$\overline{Nu} = C(Gr)^m \left(\frac{H}{L}\right)^n$$

where $\overline{Nu}$ indicates the Nusselt number describing the average heat transfer coefficient, Gr is the

Grashof number, H the height and L the thickness of the air layer. An increase in the exponent m from 1/4 to 1/3, which was found to occur at a certain Grashof number, was interpreted as indicating a transition from laminar to turbulent flow. Batchelor published in 1954 an analytical study [12] of the problem of natural convection in enclosed gas layers. He came to the conclusion that various flow regimes exist depending on the value of the Rayleigh number Ra ($Ra = Gr\,Pr$) and on the geometry. Heat is transported from the hot to the cold plate essentially by conduction when the Rayleigh number is small or moderately large and when the thickness of the fluid layer is small relative to its height. Convective effects occur in the corners of the layer only. For large Rayleigh numbers, on the other hand, boundary layers were postulated to build up along the bounding surfaces and a core of uniform temperature and vorticity was assumed to exist in the central region when the Rayleigh number approaches infinity. Batchelor also concluded from his analysis that the flow was laminar in all of the experiments, the results of which were published up to that time. A boundary layer analysis of free convection in a completely enclosed cylindrical region was performed by S. Ostrach [13]. Analytical and experimental studies of free convection in a fluid enclosed between two infinite vertical planes with locally constant heat flux at the hot and cold surface are contained in [14 and 15].

The study reported in this paper applies a Zehnder–Mach interferometer to the investigation of the temperature and flow conditions in an air layer enclosed between two vertical plates. The interferograms can be evaluated to obtain the temperature field. They also give indications of the presence or absence of velocity fluctuations and of turbulence. The existence and extent of boundary layers is clearly indicated and local heat transfer coefficients can easily be evaluated from the temperature field. In this way, a general understanding of the flow and heat transfer processes can be obtained leading to information which can be utilized for other geometries as well.

TEST APPARATUS

It was the aim to design the test apparatus for the following conditions: Two-dimensional flow and heat transfer are to be established in an air

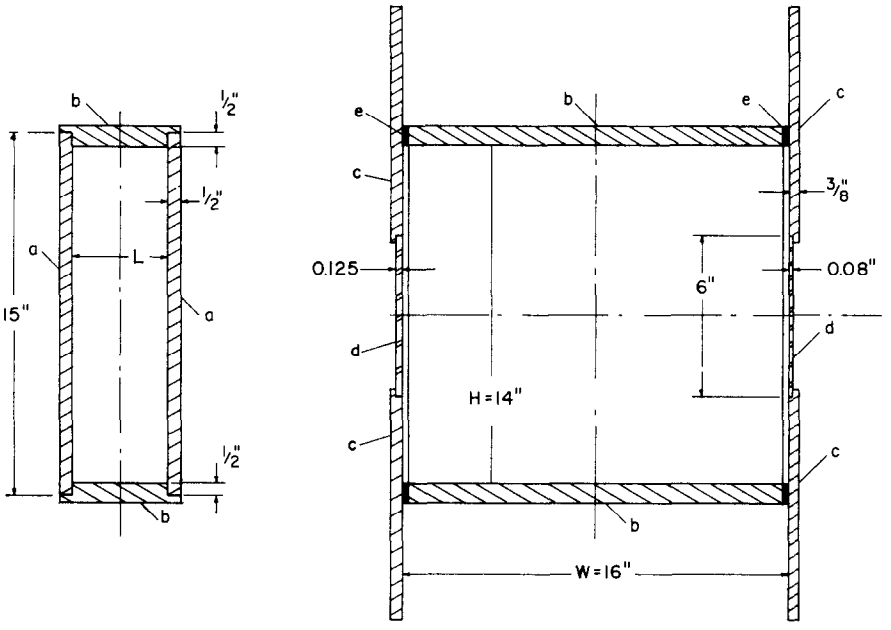

FIG. 1. Experimental setup

a copper plates, **b** balsa wood spacers, **c** balsa wood plates, **d** optical glass plates, **e** cork strips.

layer enclosed between two vertical planes. The temperatures are to be uniform over each plane, but with a different value for each of them. The horizontal walls by which the air layer is bounded are to be adiabatic to heat and mass flow. Fig. 1 gives a sketch of the apparatus in its essential features. It consists of two vertical copper plates **a** 15 in. high, 16 in. wide and 0·5 in. thick. The plates were polished and nickel-plated on the surfaces bordering on the air layer. One of the plates was heated by an electric heater consisting of a 0·005 in. × 0·125 in. Nichrom ribbon wound on a mica sheet. A second heater separated from the first one by a 0·5 in. thick balsa wood plate acted as a guard heater. The second copper plate was cooled by water running through a jacket attached to the back surface of the plate. The cooling water was kept at a constant temperature of 78°F by a Hoeppler thermostat type N. Thirteen thermocouples were inserted into each of the plates beneath the nickel-plated surface and revealed a maximum temperature variation of 3°F over the surface of the hot plate and a maximum variation of 1°F over the surface of the cold plate at a temperature difference of 160°F between both plates. The upper and lower walls **b** enclosing the air space were made of balsa wood. These spacers were available with different dimensions L. The two vertical end plates **c** were also manufactured from balsa wood. Two glass windows **d** with 6 in. diameter were inserted into these end plates so that the light beam of the interferometer could pass through the air layer. One of the glass plates was 0·08 in., the other one 0·125 in. thick. The end pieces with the glass windows could be moved in a vertical direction and in this way the air layer could be viewed through the interferometer in its whole extent. One-fourth in. thick cork strips **e** were placed between the copper plates and the end pieces in order to reduce the heating of the windows. Windows with a small thickness were chosen to avoid distortions in the interferograms caused by stresses in the glass. It was interesting to note that no extensive polishing of these glass plates was necessary because of their small thickness, but that plates with sufficient optical quality could be selected from a stock of normal optical glass plates.

The height of the air layer under investigation could be changed by additional balsa wood spacers which were clamped between the two copper plates. In this way the following heights of the layer were investigated: 14 in., 3·5 in. and 3 in. The length L was adjusted by the use of various spacers to values of 0·3 in., 0·7 in. and 1·4 in. The vertical centerline temperature profile was additionally measured at a length L of 3·75 in. and 6 in. The width W in light beam direction was 16 in. From the results of the previous work referenced in the Introduction, it was concluded that this dimension is sufficient to make end effects on the two small vertical surfaces negligible and in this way to approximate well a two-dimensional situation. An additional verification was obtained by measuring the temperatures in the air layer along a horizontal centerline parallel to the copper plates with a thermocouple probe.

The temperature difference between the hot and the cold plate was varied between 10° and 160°F at 25° intervals. Steady state conditions were established before any measurements or interferograms were taken.

The interferometer used for the study was an instrument constructed at the Heat Transfer Laboratory of the University of Minnesota, with financial support from the Graduate School of the University. It has, with a few exceptions, the same design as the instrument described in [16]. An evaluation of the interferograms results in the density field of the air layer and with the assumption of a locally uniform pressure also in the temperature field. A description of the evaluation procedure and also of a calculation of the end losses and refraction losses is contained in [1]. Both losses were found to be negligible.

The temperature in the air layer was additionally measured along vertical and horizontal centerlines with a thermocouple probe made out of No. 30 manganin- and constantan-wire. The measurements with this probe agreed well with the temperatures obtained by an evaluation of the interferograms.

The overall heat flux from the hot to the cold plate was obtained from the interferograms as well as from a measurement of the input of electric energy into the hot plate or the heat

transfered to the cooling water, after correction for the heat conduction losses, and of the radiative heat transfer. The values obtained in both ways agreed within 10 per cent. It is assumed that the evaluation of the interferograms gives the more accurate values.

TEMPERATURE FIELD

Figures 2(a)–(d) present a few samples of the interferograms taken during this study. The interferometer was, for this work, adjusted in such a way that the interference fringes were horizontal when the light beam was traveling through a field of uniform density. The fringes in Fig. 2(a) indicate, therefore, by their straightness a linear density and temperature drop in the direction from the hot to the cold plate. The lines are just slightly curved at the upper and lower corners of the air layer. Fig. 2(b) displays straight fringes in the central portion of the air layer. The fringes, however, are considerably more distorted in the corner regions. For the conditions indicated in the subscripts of the two figures, heat is therefore transported by conduction in the central part of the air layer. This does not mean that the fluid is completely at rest. It only indicates that no heat transport is connected with the flow in the central part. The distortion of the fringes and of the temperature field near the corners, however, can be attributed to convective energy transport. Fig. 2(d) displays a completely different behavior of the temperature field. There exists a layer in the central part in which the interference fringes are horizontal, indicating that the temperature is constant on horizontal lines. The temperature gradients are concentrated in two layers adjacent to the hot and the cold surfaces. This behavior of the temperature field can be interpreted as two thermal boundary layers on both vertical surfaces separated by a core with a temperature which is constant along horizontal

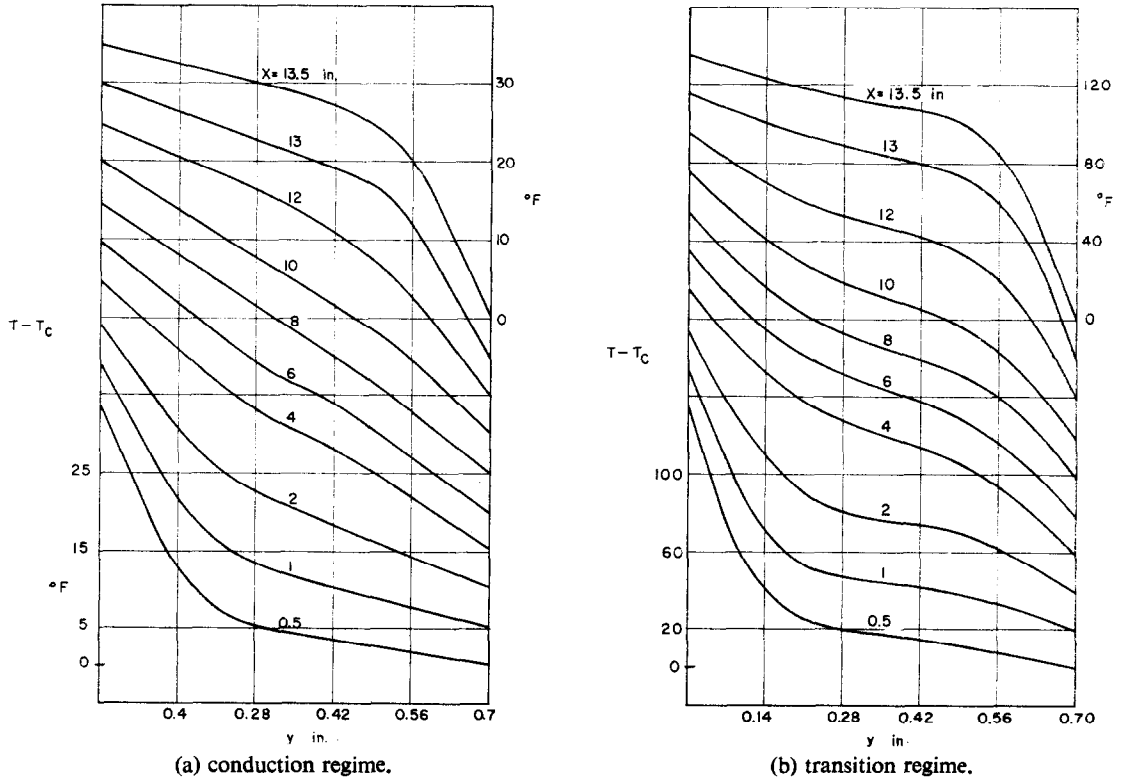

(a) conduction regime.

(b) transition regime.

FIG. 3. Temperature field in air layer with 14 in. height.

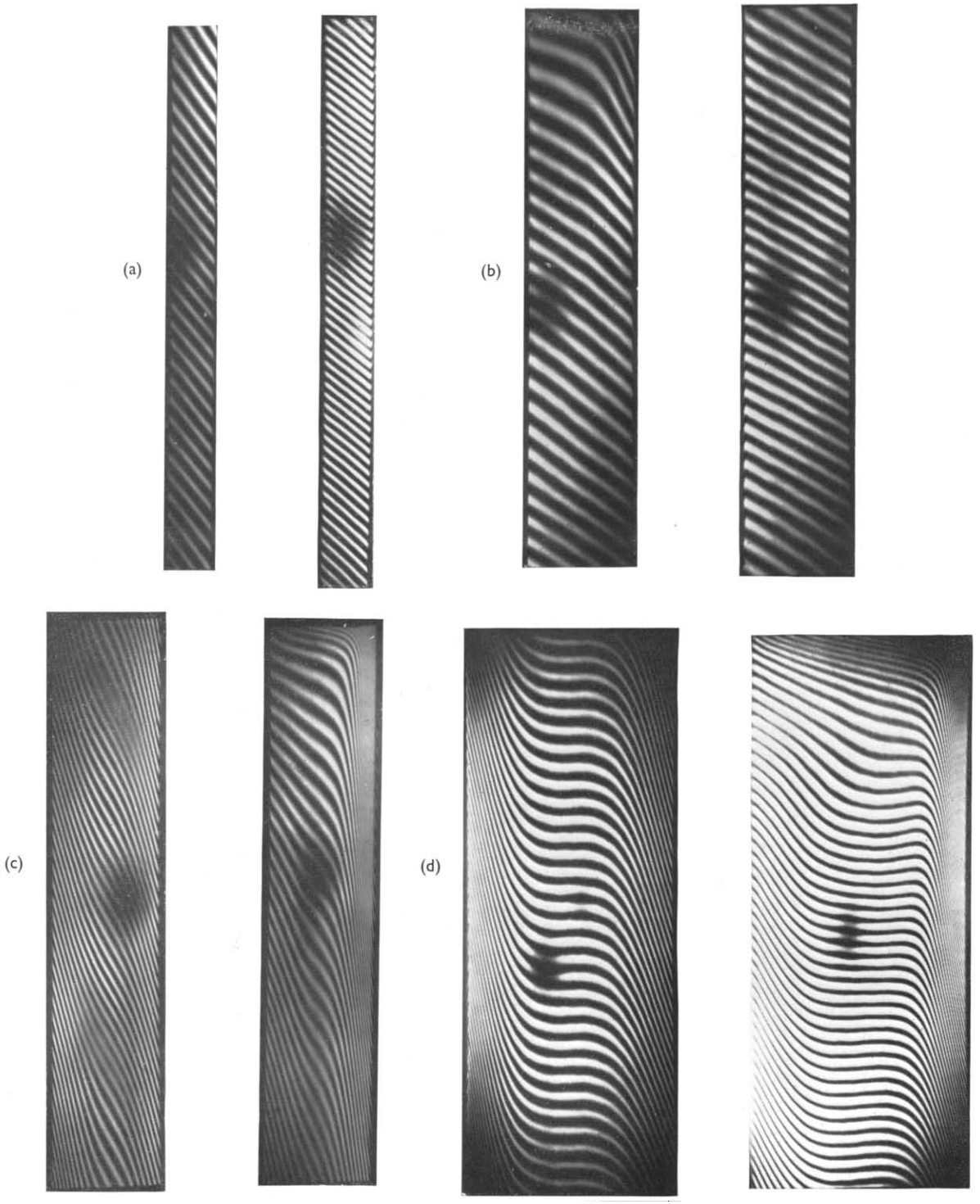

FIG. 2. Interferograms

(a) $H = 14$ in., $L = 0{\cdot}3$ in., $T_H - T_C = 10°\text{F}$
(b) $H = 14$ in., $L = 0{\cdot}7$ in., $T_H - T_C = 10°\text{F}$
(c) $H = 14$ in., $L = 0{\cdot}7$ in., $T_H - T_C = 60°\text{F}$
(d) $H = 14$ in., $L = 1{\cdot}4$ in., $T_H - T_C = 60°\text{F}$

The figures present the first and second quarter of the airspace counted from top.

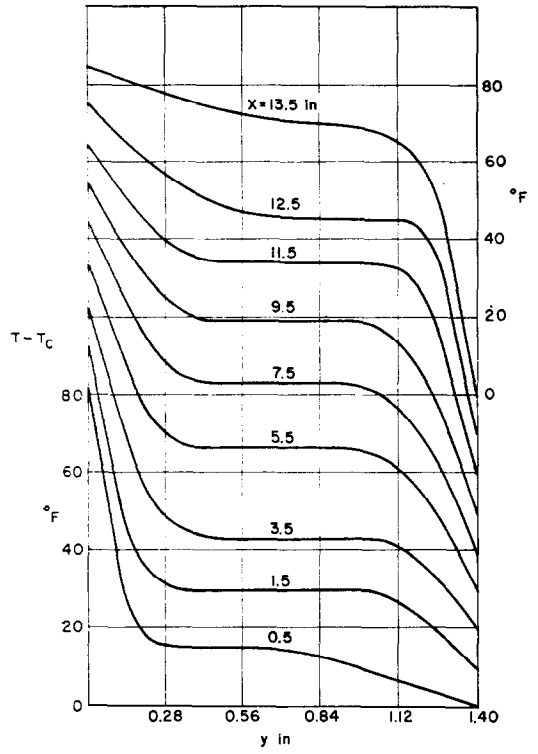

(c) boundary layer regime.

FIG. 3.—*contd.*

lines. It will be shown later on and discussed in more detail, that the temperature in the core is not constant along vertical lines. The two thermal boundary layers may not coincide with the flow boundary layers and will probably give little information on the flow field in the corners.

The temperature field is obtained quantitatively by an evaluation of the interferograms. Samples of these fields are presented in Figs. 3(a)–(c). In these figures, the local temperature T minus the temperature T_C of the cold plate is plotted over the distance y from the hot plate in inches. The temperature scales on the ordinate belong to two of the temperature profiles; the others are shifted in vertical direction. Fig. 3(a) shows a temperature field with a linear temperature drop in the center portion. Such a situation will, in the following, be referred to as the "conduction regime". Fig. 3(c), on the other hand, displays the central core with a horizontal part of the temperature profiles and the two thermal boundary layers in which the temperature gradients are concentrated. It can be observed that the boundary layer grows in thickness in an upward direction on the hot plate and in a downward direction on the cold plate. The shape of the temperature profiles in the boundary layers resembles the shape of the temperature profile arising in free convection boundary layers on a single heated or cooled plate. The conditions under which such a temperature field with a core of uniform temperature in direction along horizontal lines exists will be referred to as "boundary layer regime". Fig. 3(b) shows the temperature profiles for conditions between the boundary layer and the conduction regime. The temperature profiles are curved throughout the whole height of the air layer, indicating that convection contributes to the heat flow from the hot to the cold plate. There exists, however, no horizontal part in the profiles. In a sense one can say that the two boundary layers have met and grown together. This regime will be called "transition regime".

Figures 4(a)–(c) present the temperatures measured along a vertical line placed midway between the hot and the cold surface. The temperatures are plotted in a dimensionless way as ratio of the centerline temperature minus the cold plate temperature to the hot plate temperature minus the cold plate temperature. Fig. 4(a) shows the temperature profiles for measurements in the conduction and the transition regimes as defined before. The experimental points, indicated by crosses, have been obtained for conditions in the conduction regime. The region with a linear temperature drop from the hot to the cold plate coincides with the region in Fig. 4(a) for which the temperature parameter is equal 0·5. The other points are for measurements in the transition regime. Figs. 4(b) and (c) present the results of measurements in the boundary layer regime, one for a height to distance ratio equal 10 and the other one for $H/L = 2{\cdot}5$. It can be observed that the temperatures in the core of the air layer are by no means constant but vary approximately in a linear fashion. The temperature variation in the boundary layer regime appears not to be affected essentially by the parameter H/L. In his paper [12] Batchelor came to the conclusion that the

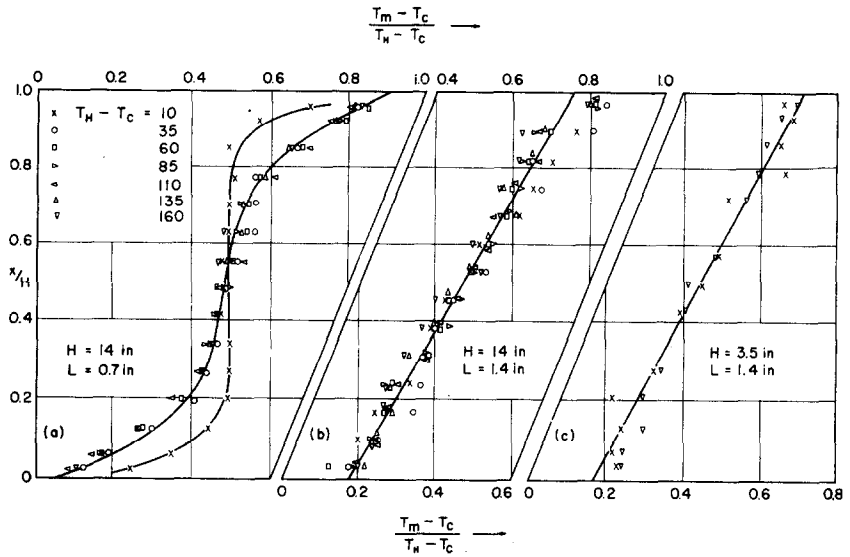

FIG. 4. Centerline temperatures.

temperature in the core is uniform for infinite Rayleigh number, and this statement was utilized in the other analytical papers as well. According to Fig. 4, this situation does not yet exist in the investigated Grashof number range. For air with a Prandtl number of 0·71, the Rayleigh number is of the same order of magnitude as the Grashof number. It may be expected that the flow within the boundary layers becomes turbulent at a Grashof number of order 10^9. It is, therefore, doubtful, whether a core of uniform temperature will ever exist together with laminar boundary layers unless the ratio H/L is very small.

It has to be expected that, for sufficiently small temperature differences, a symmetry exists in the temperature field around the midpoint in the sense that the field in the lower half of the airspace is a negative image of the field in the upper half provided the balsa wood walls are completely adiabatic to heat flow. This requires the centerline profiles in Figs. 4 to pass through the value 0·5 at the position $x/H = 0{\cdot}5$. The fact that this is not quite the case in Figs. 4(b) and (c) indicates a slight heat loss through the balsa walls or it is a consequence of the temperature dependence of the air properties.

FLOW REGIMES

The number of parameters on which local heat transfer on the hot and cold surfaces depends can be determined by dimensional analysis. This analysis predicts that a relationship of the following form exists

$$Nu = f(Gr, Pr, H/L, W/L, x/L), \qquad (1)$$

(the notation is explained in the nomenclature), if the temperature differences in the field are sufficiently small to neglect the variation of properties and for the boundary conditions and the geometry of the present investigation. It was pointed out in the Section "Test Apparatus" that the influence of the parameter W/L is negligible. The Prandtl number for air near atmospheric temperature is practically constant. The variables in the relationship (1) then reduce to

$$Nu = f(Gr, H/L, x/L). \qquad (2)$$

The form of the function f will be different for the various regimes and it is, therefore, of advantage to establish at first the limits for those. A relation of the form

$$Gr = f(H/L) \qquad (3)$$

is predicted by dimensional analysis for the limits between the various flow regimes when they are defined in the way as discussed in the previous section. The various interferograms were therefore investigated and those in which a

linear temperature drop exists in some part of the flow field are indicated by circles in Fig. 5. The conditions for which a horizontal part of the temperature profile exists at least over part of the field are indicated by crosses. The other experimental runs are indicated by squares. The number of runs is actually not sufficient to establish the limits between the various heat transfer regimes exactly. The heavy lines in the figure, however, should not be too far from the actual location of the limits. Batchelor [12] derived from various estimates the relation

$$Gr_L Pr = 500\, H/L$$

for the limit of the conduction regime. This limit is also presented in Fig. 5 as thin full line. Its location agrees fairly well with the experiments. Its slope, however, appears somewhat too small. The significance of the dashed line is

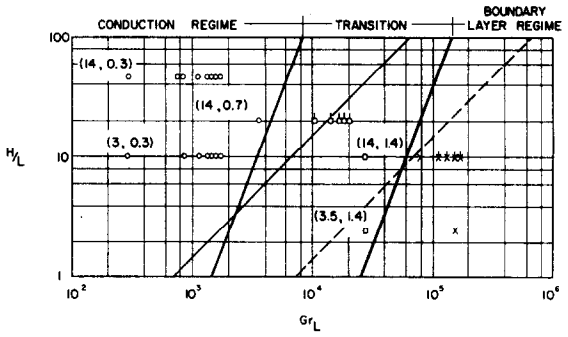

FIG. 5. Extent of various regimes.
Figures in bracket give height and thickness of air layer.

discussed in the Appendix. The Grashof number appearing on the abscissa of this figure has been based on the distance L between two plates according to the relation

$$Gr_L = \frac{g\beta(T_H - T_C)L^3}{\nu^2}. \qquad (4)$$

Turbulent fluctuations could be observed in some of the test runs. They were in most cases restricted to the core region. Runs which exhibited these fluctuations are indicated by a short line attached to the test points. It appears from inspection of Fig. 5 that the turbulent fluctuations are not connected with the establishment of the various flow regimes. The intensity of the fluctuations, however, increased in any series of runs for a fixed H/L ratio with increasing Grashof number. The fluctuations had a comparatively low frequency; in some cases regular wave motions of the form as described in [17] were also observed in the boundary layers.

HEAT TRANSFER IN CONDUCTION REGIME

This regime is characterized by the fact that heat is transferred between the two vertical plates by conduction only in the central part of the air layer. From the equation

$$q = \frac{k}{L}(T_H - T_C) = h_c(T_H - T_C) \qquad (5)$$

which defines the local heat transfer coefficient on the hot or the cold surface, the following relation

$$Nu_{L,c} = \frac{h_c L}{k} = 1 \qquad (6)$$

is obtained for the local Nusselt number in this region. $Nu_{L,c}$ can also be interpreted as ratio of an apparent conductivity of the air layer to the actual conductivity k. The evaluations from the interferograms agree very accurately with the relation (6).

The local heat transfer conditions are different in the corners of the air layer. From the symmetry of the situation pointed out before, it has to be expected that almost the same heat transfer coefficients apply for the cold and the hot plate at diagonally opposite corners. An evaluation of the interferograms showed that in one pair of corners heat transfer coefficients were larger than in the central part. These corners will be called "starting corners". They are the lower corner on the hot and the upper corner on the cold plate. In the two other corners, heat transfer coefficients were found to be smaller than in the central portion. These corners will be called "departure corners".

As long as the end effects do not penetrate to the center of the plate, it has to be expected that the local heat transfer conditions in the corners are independent of the height H of the plates. Therefore, a relation of the following form is expected to describe the local Nusselt numbers in the corners

$$Nu_x = f(Gr_x, x/L) \qquad (7)$$

with

$$Nu_x = \frac{hx}{k}, \quad Gr_x = \frac{g\beta(T_H - T_C)x^3}{\nu^2}. \tag{8}$$

Starting corners. An evaluation of the interferograms indicated that the Nusselt number Nu_x in the starting corners is independent of the ratio x/L. Figs. 6(a) and (b) present the Nusselt number Nu_x as function of the Grashof number Gr_x for the experimental runs in the conduction regime based on evaluation at the hot and at the cold plate. The experimental points can be well approximated by the following relation

$$Nu_{x,c} = 0{\cdot}256\,(Gr_x)^{0{\cdot}24} \tag{9}$$

indicated by the heavy lines in the figure. The length x on which the dimensionless parameters in this equation are based is the distance from the corner measured along the hot or cold plate surface.

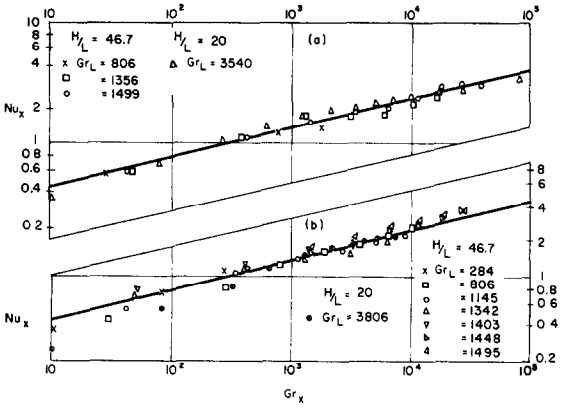

FIG. 6. Local Nusselt numbers at starting corners. (a) hot plate, (b) cold plate.

An inspection of equation (9) indicates that the heat coefficient drops with increasing distance x. The limit for the applicability of equation (9) is reached at a point where the heat transfer coefficient, determined by the equation, becomes equal to the heat transfer coefficient in the center part of the plate. The corresponding distance x_p from the corner will be called "depth of penetration". It is obtained by setting the Nusselt number Nu_x for the central part which is, according to equation (6), equal to x/L, equal to the Nusselt number as given by equation (9).

$$\frac{x_{p,s}}{L} = 0{\cdot}256\,(Gr_x)^{0{\cdot}24} = 0{\cdot}256\,(Gr_L)^{0{\cdot}24}\left(\frac{x_{p,s}}{L}\right)^{0{\cdot}24}$$

The ratio of penetration depth to distance of the plates is therefore

$$\frac{x_{p,s}}{L} = 0{\cdot}0075\,(Gr_L)^{0{\cdot}857}. \tag{10}$$

An average heat transfer coefficient for the corner region is defined by the relation

$$\bar{h}_s = \frac{1}{x_p}\int_0^{x_p} h_s \mathrm{d}x \tag{11}$$

and an average Nusselt number by

$$\overline{Nu}_{L,s} = \frac{\bar{h}_s L}{k}. \tag{12}$$

Inserting the heat transfer coefficient obtained from equation (9) into the relation (11), carrying out the integration, inserting the penetration depth from equation (10), and inserting the average heat transfer coefficient into equation (12) leads to the following expression for the average Nusselt number in the starting corner

$$\overline{Nu}_{L,s} = 1{\cdot}389. \tag{13}$$

Departure corners. An evaluation of the interferograms for the departure corner indicated that the Nusselt number Nu_x based on the distance x from the corner is, in this case, a function of the ratio x/L in addition to the Grashof number Gr_x. Figs. 7(a) and (b) present the Nusselt number Nu_x as a function of the Grashof number Gr_x. A second Grashof number Gr_L was used as parameter rather than the ratio x/L, since it is a parameter that does not depend on the local position x. The relations in Figs. 7 can reasonably well be approximated by the equation

$$Nu_{x,d} = 2{\cdot}58\,(Gr_x)^{0{\cdot}4}\,(Gr_L)^{-0{\cdot}55} \tag{14}$$

indicated by the heavy lines in the figures. This equation describes a heat transfer coefficient which is zero in the corner and increases with increasing distance x. The limit of applicability of equation (14) is again reached at a position x_p where the heat transfer coefficient described by this equation becomes equal to the heat transfer coefficient valid in the center part of the plate. The relation

$$\frac{x_{p,d}}{L} = 0{\cdot}00875\,(Gr_L)^{0{\cdot}75} \tag{15}$$

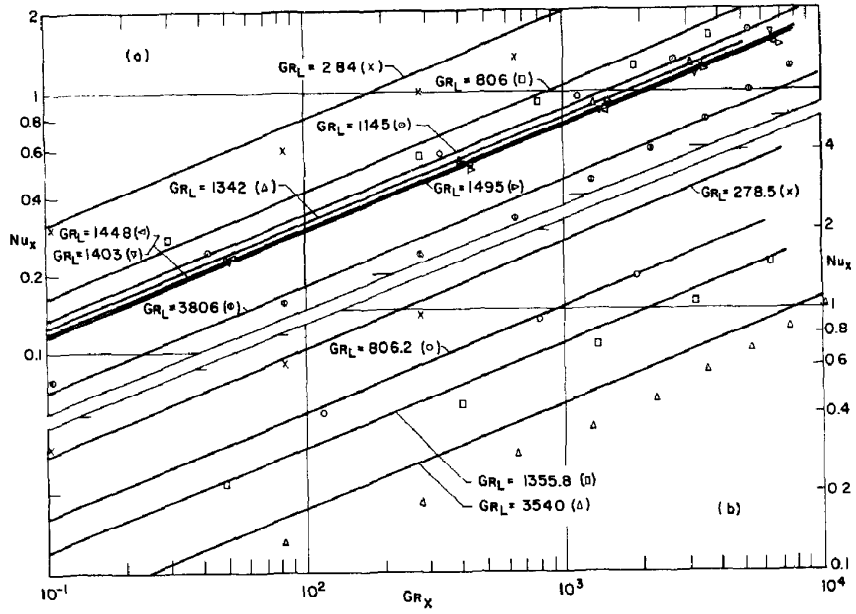

FIG. 7. Local Nusselt numbers at departure corners.
(a) hot plate, (b) cold plate.

is obtained in the same way as the one for the starting corner.

An average Nusselt number for the departure corners can also be obtained in the same way as for the starting corners. The following relation is found from the previous equations

$$\overline{Nu}_{L,d} = 0{\cdot}835.$$

Average heat transfer. The total heat flux Q from the hot to the cold plate, including the corner regions, can be obtained from the following equation

$$Q = [h_c H + (h_s - h_c)x_{p,s} + (h_d - h_c)x_{p,d}](T_H - T_C). \quad (17)$$

Changing from heat transfer coefficients to Nusselt numbers, one obtains

$$\overline{Nu}_L = \frac{QL}{kH(T_H - T_C)} =$$

$$1 + (\overline{Nu}_{L,s} - 1)\frac{x_{p,s}}{H} + (\overline{Nu}_{L,d} - 1)\frac{x_{p,d}}{H}. \quad (18)$$

Introducing the Nusselt numbers $\overline{Nu}_{L,s}$ and $\overline{Nu}_{L,d}$ from equations (13) and (16) and the penetration depths from equations (10) and (15) leads to the following relation

$$\overline{Nu}_L = 1 + \frac{L}{H}[0{\cdot}00292\,(Gr_L)^{0{\cdot}857} - 0{\cdot}00144\,(Gr_L)^{0{\cdot}75}]$$

which in the investigated Grashof number range can well be approximated by the equation

$$\overline{Nu}_L = 1 + 0{\cdot}00166\,\frac{L}{H}(Gr_L)^{0{\cdot}9}. \quad (19)$$

Batchelor [12] obtained in his analysis by a heat balance for the corner region an equation for the average Nusselt number which in the terms used in this paper reads

$$\overline{Nu}_L = 1 + \frac{2\beta - 1}{720}\,\frac{L}{H}\,Gr_L\,Pr.$$

The parameter β remains undetermined in the analysis. He estimates it to have a value close to one. This relation agrees well with the equation (19) which was derived from our experiments.

HEAT TRANSFER IN BOUNDARY LAYER REGIME

Local heat transfer. Fig. 3(c) presented the temperature field for a situation in the boundary

layer regime. It indicates that the boundary layers on the two vertical surfaces grow in a way which is similar to the behavior on a single vertical plate when the regions in the immediate neighborhood of the corner are excluded. This suggests a check whether a relation similar to the one for a single plate will describe heat transfer in the boundary layer regime of the enclosed space. A heat transfer coefficient is therefore defined by the following equation

$$q = h'(T_w - T_m) \tag{20}$$

in which T_w indicates the surface temperature of either the hot or the cold plate. T_m is the temperature in the centerline at the height x for which the heat flux q and the local heat transfer coefficient h' are defined. The distance x is in the boundary layer regime always measured from the starting corner of the plate. It increases, therefore, in the direction in which the boundary layer grows. Dimensionless Nusselt numbers and Grashof numbers are, accordingly,

$$Nu'_x = \frac{h'x}{k} \tag{21}$$

$$Gr'_x = \frac{g\beta(T_w - T_m)x^3}{\nu^2}. \tag{22}$$

Figs. 8(a)–(c) present the results of the evaluation of the experiments. Fig. 8(b) contains as points the experimental results in the boundary layer regime for an air layer with the height to thickness ratio $H/L = 10$; Fig. 8(c) shows the results for a ratio $H/L = 2{\cdot}5$. In the evaluation of the dimensionless parameters, the properties have been introduced at wall temperature. It can be observed that the experimental points in both figures correlate quite well on a single line, indicating that the parameters in equations (21) and (22) are the important ones for the boundary layer regime. No satisfactory correlation is, however, obtained when the parameters Nu_x and Gr_x are used, which are based on the temperature differences $T_H - T_C$. The correlation of the parameters Nu'_x and Gr'_x, on the other hand, holds even for the test runs in the transition regime presented in Fig. 8(a). The heavy line in the three figures which averages the experimental points has the relation

$$Nu'_x = 0{\cdot}231\,(Gr'_x)^{0{\cdot}30}. \tag{23}$$

It appears in the figure that a slightly bent line would give a somewhat better agreement with the experimental points; however, it is felt that

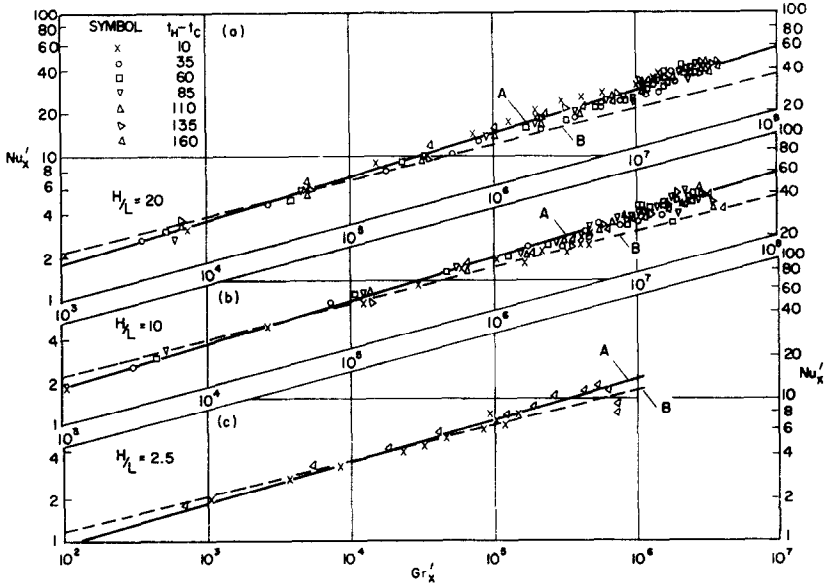

FIG. 8. Local Nusselt numbers in boundary layer and transition regime (evaluated on hot plate).
A. line averaging test points, B. flat plate relation
(a) transition regime, (b), (c) boundary layer regime.

the accuracy with which the test points correlate on a single line does not warrant to take this effect into account. The points for each test run at the lowest and highest Grashof number, especially in Fig. 8(c), lie below the curve representing equation (23). This expresses the fact that the boundary layer growth right at the corners is influenced by the corner geometry.

Equation (23) then is a relation which describes local heat transfer conditions on the heated and cooled surfaces enclosing an air layer in the boundary layer and in the transition regime. The equation can be used to calculate the local heat flux as soon as the centerline temperature is known. Fig. 9 summarizes once more the

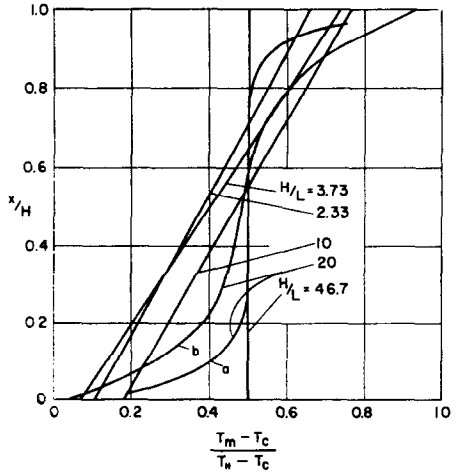

FIG. 9. Centerline temperatures
Curve (a) holds for $T_H - T_C = 10°F$, all other curves for $T_H - T_C$ from 35° to 160°F.

results of the centerline temperature measurements which have been presented before. It also includes measurements on an air layer with a height of 14 in., and with 3·75 in. and 6·0 in. thickness.

The following general features of the centerline temperature can be deduced from Figs. 4 and 9. The centerline temperature is constant for small values of Gr_L and large values of H/L throughout the whole height of the layer. With increasing Gr_L or decreasing H/L, temperature variations occur at first near the upper and lower boundaries of the layer. The centerline temperature moves closer to the hot plate temperature T_H near the upper boundary and closer to the cold plate temperature near the lower boundary. The regions of varying temperature cover a range which increases with increasing Gr_L until they meet in the center. Further on the temperature profile straightens out until it becomes practically linear within the boundary layer regime. In this regime, the centerline temperature varies with local position x in a linear way, and the thickness of the layer has a comparatively small influence.

The experimental points in Fig. 4(a) appear not to demonstrate the gradual change of the profile shape in the transition regime. This, however, is caused by the fact that the Gr_L variation in the tests with $T_H - T_C$ between 35° and 160°F is only a small part of the whole Gr_L range in the transition regime.

The shape of the temperature field in the conduction and in the boundary layer regimes explains a peculiar behavior of the heat flow through enclosed vertical air layers which has been predicted by Batchelor [12] and found experimentally by E. Schmidt [18]. It was found that for a vertical air layer, enclosed by a cooled and a heated vertical plane, the heat flux increased when the air layer was subdivided into smaller cells by thin horizontal partitions. This observation can be explained by the fact that the horizontal partitions cause heat to be transported by convection in the conduction regime and new thermal boundary layers to start on the hot and cold surfaces in the boundary layer regime. The average boundary layer thickness in the space with partitions will, therefore, be smaller than when the partitions are left off.

Dashed lines have been inserted into Fig. 8. They represent the relation describing laminar free convection heat transfer on a single vertical plate in an infinite surrounding of constant temperature [Ref. 19, p. 315]. Equations (20) to (22) have been used to define the heat transfer parameters and the correct measured value T_m was introduced for each location x. It can be observed that the correlation for the enclosed space indicates higher Nusselt numbers, especially for larger Grashof numbers. This can have its reason in a beginning turbulence or, more probably, in the fact that the core of the fluid has not a uniform temperature and that the flow

boundary layer develops in a way that is different from the situation on a single plate. This one can prove simply by a continuity consideration.

Average heat transfer. An average heat transfer coefficient can be calculated from equation (23) for the boundary layer region. With the definitions

$$\overline{Nu}_H = \frac{\bar{h}H}{k} \qquad \bar{h}(T_H - T_C) = 1/H \int_0^H q\mathrm{d}x. \quad (24)$$

there is obtained

$$\overline{Nu}_H = \frac{1}{k(T_H - T_C)} \int_0^H q\mathrm{d}x = \int_0^H \frac{Nu'_x}{x} \frac{T_H - T_m}{T_H - T_C} \mathrm{d}x. \quad (25)$$

The centerline temperature parameter in Fig. 4(b) can be approximated by the equation

$$\frac{T_H - T_m}{T_H - T_C} = 0{\cdot}83 - 0{\cdot}60 \frac{x}{H}. \quad (26)$$

Introduction of this relation and of equation (23) into equation (25) leads to

$$\overline{Nu}_H = 0{\cdot}119\,(Gr_H)^{0{\cdot}3}. \quad (27)$$

Batchelor [12] estimated the rate of heat transfer in the boundary layer region and obtained the relation

$$Nu_H = C\,(Gr_H)^{1/4}$$

with values 0·38 and 0·48 for the constant C. The difference between this equation and equation (27) is probably due to the fact that Batchelor assumed a core with uniform temperature.

In terms of the parameters Nu_L and Gr_L the equation (27) reads

$$Nu_L = 0{\cdot}119\,(Gr_L)^{0{\cdot}3} \left(\frac{L}{H}\right)^{0{\cdot}1}.$$

This relation indicates a small effect of the height to thickness ratio on Nu_L or the equivalent ratio k_a/k of apparent conductivity to true conductivity of the fluid. The heat transfer coefficients calculated with this equation agree within approximately 20 per cent with previous measurements [4]. It has to be kept in mind that the equation (27) holds only for the boundary layer regime because of the linear relation for the centerline temperature which was used in the integration.

The exponent in equation (23) might suggest that the flow in the boundary layers is turbulent. This, however, does not agree with the visual observation of the temperature field as outlined before. We assume rather that the temperature variation in the core of the fluid is responsible for the relatively high value of the exponent.

APPENDIX I

A first order determination of the limit between the conduction regime and the boundary layer regime can be based on the assumption that this limit occurs when the two boundary layers on the hot and cold surfaces meet somewhere within the air layer. Since only an order of magnitude determination is desired, a relation for the boundary layer thickness may be used which holds for a single vertical surface. The local heat transfer for a vertical plate of constant temperature in an infinite environment is, according to E. Schmidt and W. Beckmann, described by the following relation [Ref. 19, p. 315].

$$Nu_x = 0{\cdot}360\,(Gr_x)^{1/4} \quad (28)$$

for air with a Prandtl number equal 0·714. The boundary layer thickness is connected with the Nusselt number by the following relation

$$Nu_x = 2\frac{x}{\delta}$$

if the temperature profile is approximated by a parabola [Ref. 19, p. 315]. Assuming that the two boundary layers meet at an x value which is half the height H of the air layer, the following relations will hold

$$x = \frac{H}{2}, \quad \delta = \frac{L}{2}.$$

From the above equations, it follows that

$$\frac{2H}{L} = 0{\cdot}360 \frac{(Gr_H)^{1/4}}{2^{3/4}} = 0{\cdot}214\,(Gr_L)^{1/4} \left(\frac{H}{L}\right)^{3/4}.$$

The height to thickness ratio finally is

$$\frac{H}{L} = 1{\cdot}32 \times 10^{-4}\, Gr_L. \qquad (29)$$

This relation is inserted in Fig. 5 as a dashed line. It may be observed that this line generally agrees quite well with the average for the limits between conduction and mixed regime and between mixed and boundary layer regime. The dashed line, however, is definitely more inclined than the limits obtained from the measurements.

APPENDIX II

Batchelor pointed out [12] that the following heat balance has to be fulfilled for the corner region of the air space in the conduction regime.

$$Q_{cv} = Q_s - Q_d$$

Q_{cv} is the enthalpy carried by convection through a plane 1–1 (Fig. 10) arranged sufficiently far from the corner to make end effects negligible. Q_s is the heat flux entering the plate in the starting corner region (in Fig. 10 the cold plate)

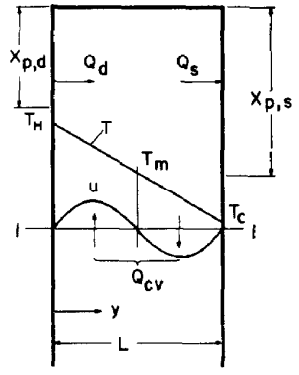

FIG. 10. Sketch of upper end of layer with temperature and velocity field in conduction regime.

and Q_d is the heat flux leaving the plate in the departure corner region (in Fig. 10 the hot plate). The temperature profile along 1–1 is given by

$$T - T_m = (T_H - T_C)\left(\frac{1}{2} - \frac{y}{L}\right).$$

The velocity profile along 1–1 is, according to Batchelor [12],

$$u = \frac{\alpha}{L}\frac{Ra}{12}\frac{y}{L}\left(1 - \frac{y}{L}\right)\left(1 - 2\frac{y}{L}\right).$$

Its shape is indicated in Fig. 10. The convective transport per unit width W can be expressed by the equation

$$Q_{cv} = \rho c_p \left(\int_0^{L/2} T u dy + \int_{L/2}^{L} T u dy\right) =$$

$$\rho c_p \left[\int_0^{L/2} (T - T_m) u dy + \int_{L/2}^{L} (T - T_m) u dy\right]$$

$$= 2\rho c_p \int_0^{L/2} (T - T_m) u dy.$$

Introduction of the above expressions for T and u and integration results in

$$Q_{cv} = k\frac{Ra}{720}(T_H - T_C).$$

The conductive heat fluxes may be obtained from equations (9) and (14). One obtains by integration

$$Q_s - Q_d = k\,(0{\cdot}00292\, Gr_L^{0{\cdot}857} + 0{\cdot}00144\, Gr_L^{0{\cdot}75})\,(T_H - T_C)$$

when the distance of plane 1–1 from the end of the air space is chosen equal to or larger than the penetration depth $x_{p,s}$ (Fig. 10).

For a Prandtl number 0·72 and a Grashof number $Gr_L = 10^3$, the convective heat flux is

$$Q_{cv} = k(T_H - T_C)$$

and the difference of the conductive fluxes is

$$Q_s - Q_d = 1{\cdot}34\, k(T_H - T_C).$$

The heat balance appears, therefore, reasonably well fulfilled, especially when it is kept in mind that for larger Gr numbers the agreement becomes even better.

REFERENCES

1. W. O. CARLSON, *Interferometric Studies of Convective Flow Phenomena in Vertical Plane Enclosed Air Layers*. Ph.D. Thesis, Graduate School, University of Minnesota (1956).
2. W. NUSSELT, *V.D.I. ForschArb.* Nos. 63 and 64, 78 (1909).
3. E. SCHMIDT, *Z., V.D.I.* 71, 1396 (1927).
4. W. MULL and H. REIHER, *Beih. Gesundh.-Ing.* Reihe 1, Heft 28 (1930).

5. E. F. M. VAN DER HELD, *Warmtetechniek* **2**, (1931).
6. E. R. QUEER, *Trans. Amer. Soc. Heat. Vent. Engrs.* **38**, 77 (1932).
7. G. B. WILKES and C. M. F. PETERSON, *Heat. Pip. Air Condit.* **9**, 505 (1937).
8. MAX JAKOB, *Trans. Amer. Soc. Mech. Engrs.* **68**, 189 (1946).
9. R. E. PECK, W. S. FAGAN and P. P. WERLEIN, *Trans. Amer. Soc. Mech. Engrs.* **73**, 281 (1951).
10. J. G. A. DE GRAAF and E. F. M. VAN DER HELD, *Appl. Sci. Res.* **3**, 393 (1953).
11. H. E. ROBINSON and F. J. POWLITCH, *The Thermal Insulating Value of Airspaces.* Housing Research Paper No. 32, Housing and Home Finance Agency, Washington, D.C., April, 1954.
12. G. K. BATCHELOR, *Quart. Appl. Math.* **12**, 209 (1954).
13. S. OSTRACH, *A Boundary Layer Problem in the Theory of Free Convection.* Ph.D. Thesis, Graduate School, Brown University, 1950, referenced in G. F. CARRIER, *Boundary Layer Problems in Applied Mechanics* **3**, p. 1, Academic Press (1953).
14. S. OSTRACH, *Combined Natural and Forced-Convection Laminar Flow and Heat Transfer of Fluids With and Without Heat Sources in Channels with Linearly Varying Wall Temperatures.* Nat. Advisory Comm. of Aeronautics, TN 3141 (1954).
15. A. F. LIETZKE, *Theoretical and Experimental Investigation of Heat Transfer by Laminar Natural Convection Between Parallel Plates.* Natl. Advisory Comm. of Aeronautics, Report 1223 (1955).
16. E. ECKERT, R. DRAKE and E. SOEHNGEN, *Manufacture of a Zehnder–Mach Interferometer.* United States Air Force, Wright–Patterson Air Force Base, Dayton, Ohio, TR 5721 (1948).
17. E. R. G. ECKERT, E. SOEHNGEN and P. J. SCHNEIDER, 50 *Jahre Grenzschichtforschung*, p. 407, Vieweg and Sohn, Braunschweig (1955).
18. E. SCHMIDT, *Chem.-Ing.-Tech.* **28**, 175 (1956).
19. E. R. G. ECKERT and R. M. DRAKE, JR., *Heat and Mass Transfer*, 2nd edition. McGraw-Hill, New York (1959).